Three-Dimensional Optical Coherence Tomography Employing a 2-Axis Microelectromechanical Scanning Mirror

Woonggyu Jung, Jun Zhang, Lei Wang, Petra Wilder-Smith, Zhongping Chen, *Member, IEEE*, Daniel T. McCormick, and Norman C. Tien, *Member, IEEE*

***Abstract*—We present a three-dimensional (3-D) optical coherence tomography (OCT) system based on a dual axis microelectromechanical system (MEMS) mirror. The MEMS mirror provides high-speed, high resolution 2-axis scanning while occupying a very small volume with extremely low power consumption. The dimensions of the mirror are 600 × 600 μm, and both axes are capable of scanning up to 30 degree angles at frequencies greater than 3 kHz with good linearity. A 3-D image set is acquired when the MEMS mirror is integrated with the fiber-based OCT system. Via 2-axis lateral scanning, combined with an axial scan, a volume (2 × 2 × 1.4 mm) image of tissue, including a cancerous region, from a hamster cheek pouch was obtained. Using a signal processing technique, image data is normally presented by 3-volume showing views at arbitrary angles and locations. The objective of this work is to show the capabilities of a 3-D OCT system utilizing a MEMS scanner as this technology can readily by applied to realize OCT beam delivery systems such as hand held scanners and endoscopic probes. A MEMS based 3-D OCT system employing a high speed, small volume scanner may have the potential to expand the application area of OCT and revolutionize areas of clinical medicine as well as medical research.**

***Index Terms*—2-axis miceoelectromechanical scanning mirror, three-dimensional optical coherence tomography (3D OCT).**

I. Introduction

OPTICAL coherence tomography (OCT) is a well known technique capable of performing cross sectional imaging. Shortly following its invention, OCT became an attractive technology in medical imaging because of several advantages, such as high spatial resolution, noninvasiveness, and real time measurement [1]–[4]. OCT research has focused on many applications in the fields of biology and biomedicine. However, in many cases, two-dimensional (2-D) OCT is not sufficient to fully describe and visualize morphological changes, or to determine margins of diseased tissue. For example, it is difficult to find early cancerous regions in tissue with only 2-D OCT images. It is also hard to estimate the extent of cancer and determine its precise stage. Therefore, 3-D imaging is required to improve the performance of OCT in many clinical cases.

For this reason, many research groups have worked and reported on 3-D OCT images [5]–[10]. Previous research efforts have primarily been focused within two categories: the 2-D scanning method itself, and improvement of system speed to obtain 3-D images. The representative scanning method for 3-D OCT is a raster scanning technique, which utilizes a combination of two 1-D scanners [5], [6]. This method has the advantage of simple design. However, it has restrictions in terms of both size and scanning speed, as well as the introduction of an additional image plane. Whereas advanced techniques using a charge coupled devices (CCD) camera and smart detector array, such as parallel OCT, show accessible 3-D data acquisition time, they also have a disadvantage of large size which impedes their adaptation to many clinical applications [7]–[10]. A 3-D technique for both fast data acquisition and compactness of the scanner is essential, because fast data acquisition reduces moving artifacts such as breathing during scanning, and a small size scanner provides easy access to the imaging site using a handheld probe or endoscope. With recent advances in frequency domain OCT (FD-OCT) techniques, axial scan speed as high as 40 kHz have been demonstrated [11]–[13]. Therefore, a high speed and compact 2-D scanner is required for achieving a 3-D image.

Recently, MEMS based systems have received extensive attention and found numerous applications in biomedical instrumentation because of many advantages, including low power consumption, small size, precise feature control and high operation speeds. Micromachined scanning probes are capable of providing fast speed, low power, and high reliability scanning in a compact package that can be used for endoscopic OCT imaging [14]–[17].

In this paper, we report the use of MEMS technology for 3-D OCT imaging. The bench-top based MEMS scanner was developed and incorporated with time domain OCT (TD-OCT) system. The design and characterization of the two axis MEMS mirror are described and 3-D images of cancer in hamster cheek pouch tissue are presented. The acquired 3-D image allows arbitrary sectioning along any x–y, x–z, and y–z axis to be displayed. Additional image processing or animation may be applied to provide specific information to the viewer.

Manuscript received March 8, 2005; revised July 25, 2005 and August 8, 2005. This work was supported by research grants awarded from the National Science Foundation (BES-86924), California Tobacco Related Disease Research Program (14IT-0097), and National Institutes of Health (EB-00293, NCI-91717, RR-01192), the Air Force Office of Scientific Research (F49620-00-1-0371, FA9550-04-1-0101, CRFA 30003, CCRP 00-01391V-20235), and the Beckman Laser Institute.

W. Jung and Z. Chen are with the Beckman Laser Institute, and the Department of Biomedical Engineering, University of California, Irvine CA 92717 USA (e-mail: jungw@uci.edu; z2chen@uci.edu).

J. Zhang, L. Wang, and P. Wilder-Smith are with the Beckman Laser Institute, University of California, Irvine CA 92717 USA.

D. T. McCormick and N. C. Tien are with the Berkeley Sensor and Actuator Center; the Department of Electrical Engineering and Computer Science, University of California, Berkeley CA 94720 USA, and also the Department of Electrical and Computer Engineering, University of California, Davis, CA 95616 USA.

Digital Object Identifier 10.1109/JSTQE.2005.857683

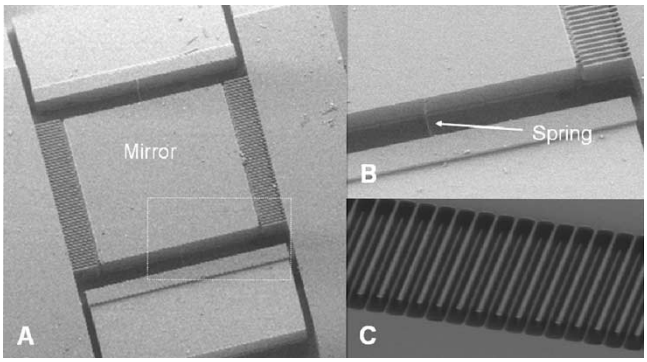

Fig. 1. (a) 600×600 μm mirror is shown. The device is 20 μm thick with 5 μm thinned comb fingers. (b) A side profile of the anchor, spring, fingers and mirror contact are shown. (c) Asymmetric fingers are shown in a top view.

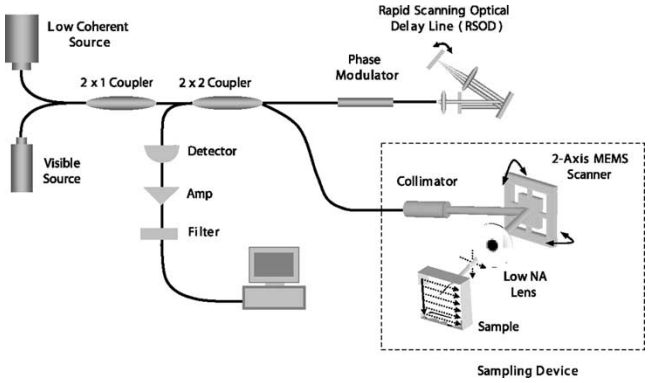

Fig. 2. Schematic of OCT imaging system: RSOD, rapid-scanning optical delay. Dotted line indicates beam delivery which is based on the 2-axis MEMS scanner and collimator. A 3-D image set is acquired when a MEMS mirror is integrated with the fiber based OCT system.

II. Method

The MEMS mirror employed in this work was a 2-D monolithic scanner fabricated from single crystal silicon. A thin (approximately 2 μm) mirror membrane was supported by a backbone of 20 μm stiffening trusses which eliminated undesired modes and dynamic deformation while minimizing the mirror's inertia. Furthermore, localized masses were incorporated for mechanical response control. The size of the mirror element was 600×600 μm and the MEMS die occupied a volume of $2.5 \times 3 \times 0.5$ mm; the reflecting surface was coated with approximately 100 nm of evaporated gold to improve the reflectance at 1310 nm. When voltage is applied on the multilayer vertical electrostatic comb-drives, mirror is actuated up and down along the spring in the both axes. The multilevel fingers provide capacitive position sensing as well as actuation capability. The maximum drive voltage in this experiment was 100 V. The device is driven such that a linear scan with constant velocity, i.e. constant dwell time at each imaging point, is achieved. The waveform employed to drive the voltage is computed from the measured response of the specific device and stored in a look-up-table. This waveform is then applied to the device and the accuracy as well as precision of the scan is verified employing a position sensitive diode (PSD) and optical feedback system. The amplifier driving the devices delivered a maximum voltage of 150 V during drive transients; however, the electrostatic comb-structures require very small currents and charge quantities in order to operate and the amplifier incorporates protective circuitry at the output. While operation of the mirror was optimized at resonance, the device may also be driven off resonance in an open or closed loop configuration. Mirrors were characterized using both capacitive and optical feedback prior to incorporation with the OCT system. The mirror employed in this work exhibited x and y-axis resonant frequencies of 8 kHz and 3.5 kHz, respectively. Within this frequency range, the MEMS scanner operated with good linearity and stability with scan angles of 30° [18]. Fig. 1 shows the scanning electron microscope image of the scanner. Fig. 1(a) presents only one axis, but the other axis is also located outside with exactly the same structure. The spring and comb-driver are magnified in Fig. 1(B) and (C).

The 2-D MEMS scanner was integrated with a fiber based OCT system as shown in Fig. 2. The system used a low-coherence length light source that delivered an output power of 10 mW at a central wavelength of 1310 nm with a bandwidth of 80 nm, providing 10 μm axial resolution. A visible aiming beam (633 nm) was used to locate the exact position and path on the sample, and both light sources were coupled into a fiber-based Michelson interferometer. In the reference arm, a rapid-scanning optical delay line (RSOD) was used that employed a grating to control the phase and group delays separately so that no phase modulation was introduced when the group delay was scanned [3], [19]. The phase modulation was generated through an electro-optic phase modulator that produced a carrier frequency. The axial line scanning rate was 500 Hz and the modulation frequency was 500 kHz. In the sampling arm, the previously described MEMS scanner was employed to provide sample scanning; the MEMS device was controlled by custom electronics interfaced to the OCT data acquisition system. The light from the fiber was coupled into a $\phi 500$ μm collimator, deflected by the MEMS mirror, and then focused by the lens ($\phi 7$ mm) with 10 mm focal length and 20 μm spot size on the image plane. 2-D cross-sectional images were acquired by one axis scanning of the MEMS scanner sequentially after each axial scanning of RSOD. In an analagous manner, a 3-D image set was obtained by a combination of the transverse scans (y) and the longitudinal scans (x) by the MEMS scanner, as well as axial scans (z) at 500 Hz by the RSOD of the reference arm. Fig. 3 presents a scanning sequence by the scanning of the MEMS mirror. Normally, scanning speed along the y axis was faster than the scan of the x axis. However, both the transverse and the longitudinal scans of the MEMS scanner were synchronized with the axial scanning of the RSOD. This scanning methodology is identical to raster scanning achieved by a pair of 1-D scanners; however, the 2-D scanning achieved by a single device eliminates an image plane and is significantly more compact. Fig. 4 presents a photograph of a scanning mirror packaged for bench-top characterization and testing as well as various scan patterns with a visible light source to demonstrate the flexibility of the MEMS scanner.

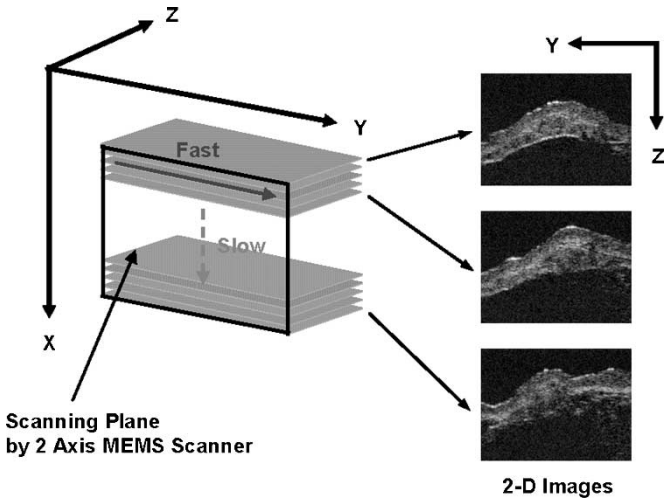

Fig. 3. Scanning sequence by the scanning of MEMS mirror. 2-D cross-sectional images were acquired by one axis scanning of the MEMS scanner along the lateral direction (solid arrow depicts the y axis scan) sequentially after each depth scanning of RSOD (along z axis). In an analagous manner, a 3-D image set was obtained by a combination of the transverse scans (y), the longitudinal scans (along the x axis: dotted arrow) by the MEMS scanner, and axial scans (z) at 500 Hz by the RSOD of the reference arm. Transverse scan are performed faster than longitudinal scan, but both scans of the MEMS scanner were synchronized with the axial scanning.

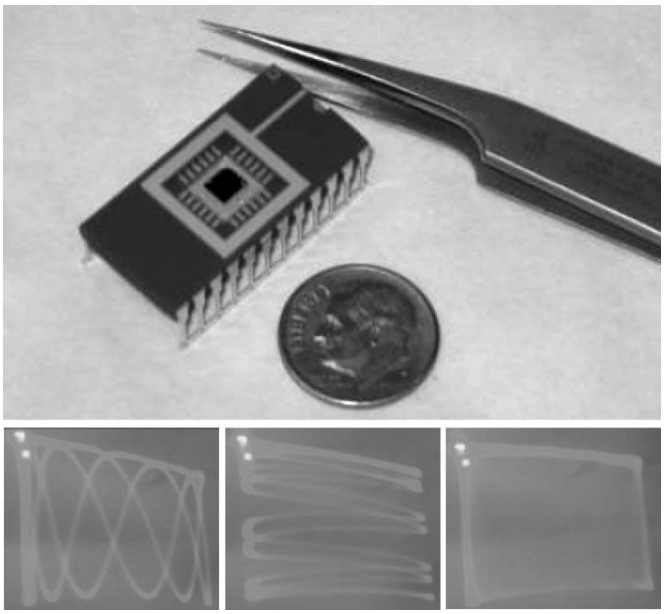

Fig. 4. (*Top*) A photograph of a 2-D MEMS scanning mirror packaged in a standard 24 pin DIP for characterization and bench-top testing. (*Bottom*) Flexibility of scanning pattern by the 2-axis MEMS scanner is presented. The various scanning patterns can be acquired by applying different frequency (or arbitrary) waveforms to each axis.

The reflected beams from the sample and reference arms were recombined in the interferometer and detected with a photodetector. Interference signals were observed only when the optical path length differences of the two interferometer arms were matched within the source coherence path length. The detected optical interference fringe intensity signals were filtered at the carrier frequency, and the resultant signals were displayed as

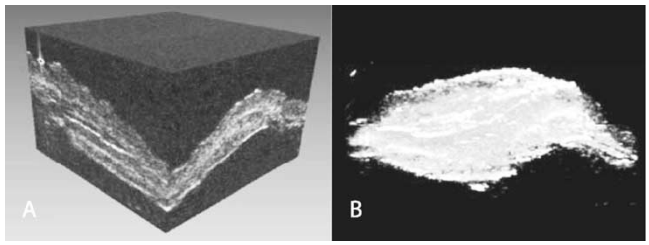

Fig. 5. The reconstructed 3-D image acquired in a normal hamster cheek pouch. (a) The 3-D image has volume ($2 \times 2 \times 1.4$ mm) and provides detailed information on tissue such as epithelium, mucosa, and submucosa. (b) The result after image processing by the threshold value.

2-D images after signal processing. For 3-D images, sequential 2-D images were continuously saved and displayed in real time during scanning. As previously mentioned, in order to acquire a complete 3-D OCT image, each scanning point visited by the MEMS mirror requires depth scanning by a rapid-scanning optical delay line (RSOD). With the current 500 Hz depth scanning speed, 3-D images were achieved at 3–5 frames/s. When the full 3-D scan was completed, the collected data was reconstructed to generate a 3-D volume image. The 3-D volume image is visualized using dedicated software; image processing, such as thresholding, iso-surface extraction, and false coloring, was employed to extract specific information.

III. Results

Fig. 5 demonstrates a reconstructed 3-D image acquired in a normal hamster cheek pouch. By 2-axis scanning, 200 images with a 10 μm span were saved, and a 3-D volume was then generated from original images. The 3-D image presented in Fig. 5(a) has volume ($2 \times 2 \times 1.4$ mm). The 3-D image provides detailed information about tissue such as epithelium, mucosa, and submucosa. It showed not only one image plane, but also successive adjacent image planes. However, in order to obtain only entire tissue structure, a volume image in a box shape requires further image processing. For this purpose, a threshold value was assigned in the 3-D volume, and background was removed. Fig. 5(b) illustrates the post-imaging processed result of Fig. 5(a). Fig. 5(b) shows clear morphology and is able to give useful structural information at any location of interest.

The MEMS OCT system was used in clinical study on cancer detection. Results are presented in Fig. 6. Fig. 6(a) is an image that combines a 2-D image and a 3-D volume image ($2 \times 2 \times 1.4$ mm). At the edge of Fig. 6(a), a good match between the original 2-D OCT image and the thresholded volume was observed. In this image, strata, such as epithelium and mucosa are clearly observed in each plane. Fig. 6(b)–(d) present 3-D volumes images at different angles to provide a better visualization of tissue structure. On the surface of Fig. 6(b), early cancer was visualized with a vivid border and distinguished very clearly from a normal region. As previously mentioned, it is difficult to detect early cancerous regions in tissue and to estimate the extent of cancer using 2-D image. In contrast to the 2-D image, the 3-D image is able to delineate the basement membrane location and configuration clearly, which is an important diagnostic criteria

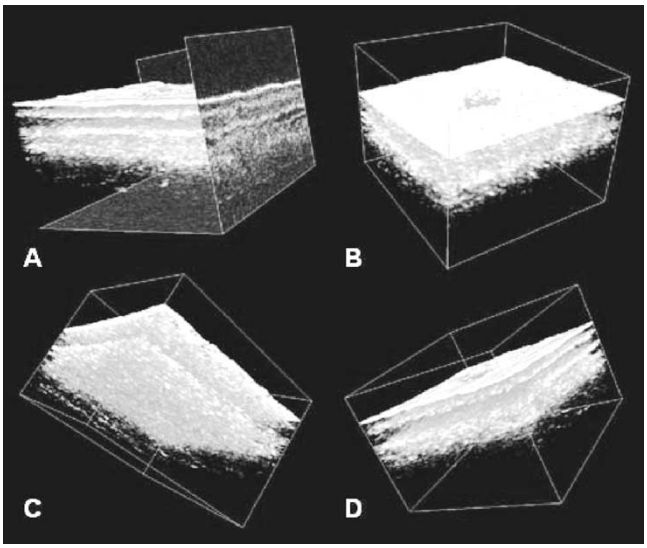

Fig. 6. Constructed 3-D volume image ($2 \times 2 \times 1.4$ mm) from the cancerous hamster cheek pouch. (a) Combination with a 2-D image and a 3-D volume image. (b)–(d) 3-D volume image at different angle to get a better visualization. On the surface of the figures, early cancer is visualized with a vivid border and distinguished very clearly from normal region. The basement, membrane which is important evidence for cancer diagnosis, is observed at the different plane.

for malignancy. Therefore, this representation goes far beyond 2-D tomographic images and is useful for localizing regions of particular interest.

IV. Conclusion

We have presented a 3-D OCT imaging system employing a 2-axis MEMS scanner. The system was used to obtain 3-D images of hamster cheek pouch tissue. The reconstructed volume images provide high resolution, detailed information about tissue physiology and health as well as clear visualization of layered structures. In particular, in the reconstructed cancerous 3-D image, the basement membrane, which is a very important indicator of dystplastic and malignant change, was clearly distinguished. Our results provide useful information to clinicians because not only 2-D images of a single tomographic slice are presented but also visualization of adjacent tissue thereby allowing identification of dynamic phenomena throughout the entire volume. The OCT system based on MEMS scanning technology has additional advantages due to the fact the MEMS device exhibits dramatic improvements in terms of both size and speed performance. Therefore, it may be a potential method to realize miniature endoscopic or catheter OCT probes. Since neither the optical resolution limits nor speed limits of the current MEMS based probe have been reached in our existing TD-OCT setup, better resolution and faster image speed could be also achieved if high resolution FD-OCT system is integrated with the MEMS devices.

References

[1] D. Huang, E. A. Swanson, C. P. Lin, J. S. Schuman, W. G. Stinson, W. Chang, M. R. Hee, T. Flotte, K. Gregory, C. A. Puliafito, and J. G. Fujimoto, "Optical coherence tomography," *Science*, vol. 254, pp. 1178–1181, 1991.

[2] A. F. Fercher, "Optical coherence tomography," *J. Biomed. Opt.*, vol. 1, pp. 157–173, 1996.

[3] A. M. Rollins, M. D. Kulkarni, S. Yazdanfar, R. Ungarunyawee, and J. A. Izatt, "*In vivo* video rate optical coherence tomography," *Opt. Express*, vol. 6, pp. 219–229, 1998.

[4] J. M. Schmitt, "Optical coherence tomography (OCT): A review," *IEEE J. Sel. Top. Quantum Electron.*, vol. 7, pp. 931–935, 2001.

[5] A. G. Podoleanu, M. Seeger, G. M. Dobre, D. J. Webb, D. A. Jackson, and F. W. Fitzke, "Transversal and longitudinal images from retina of the living eye using low coherence reflectometry," *J. Biomed. Opt.*, vol. 3, pp. 12–20, 1998.

[6] B. M. Hoeling, A. D. Fernandez, R. C. Haskell, E. Huang, W. R. Myers, D. C. Petersen, S. E. Ungersma, R. Y. Wang, M. E. Williams, and S. E. Fraser, "An optical coherence microscope for 3-dimensional imaging in developmental biology," *Opt. Express*, vol. 6, pp. 136–146, 2000.

[7] E. Beaurepaire, A. C. Boccara, M. Lebec, L. Blanchot, and H. Saint-Jalmes, "Full-field optical coherence microscopy," *Opt. Lett.*, vol. 23, pp. 244–246, 1998.

[8] A. Knüttel, J. M. Schmitt, and J. R. Knutson, "Low-coherence reflectometry for stationary lateral and depth profiling with acousto-optic deflectors and a CCD camera," *Opt. Lett.*, vol. 19, pp. 302–304, 1994.

[9] S. Bourquin, P. Seitz, and R. P. Salathé, "Optical coherence topography based on a two-dimensional smart detector array," *Opt. Lett.*, vol. 26, pp. 512–514, 2001.

[10] M. Laubscher, M. Ducros, B. Karamata, T. Lasser, and R. Salathé, "Video-rate three-dimensional optical coherence tomography," *Opt. Express*, vol. 10, pp. 429–435, 2002.

[11] S. H. Yun, G. J. Tearney, B. E. Bouma, B. H. Park, and J. F. de Boer, "High-speed spectral-domain optical coherence tomography at 1.3 μm wavelength," *Opt. Express*, vol. 11, pp. 3598–3604, 2003.

[12] R. A. Leitgeb, W. Drexler, A. Unterhuber, B. Hermann, T. Bajraszewski, T. Le, A. Stingl, and A. F. Fercher, "Ultrahigh resolution Fourier domain optical coherence tomography," *Opt. Express*, vol. 12, pp. 2156–2165, 2004.

[13] J. Zhang, J. S. Nelson, and Z. Chen, "Removal of a mirror image and enhancement of the signal-to-noise ratio in Fourier-domain optical coherence tomography using an electro-optic phase modulator," *Opt. Lett.*, vol. 30, pp. 147–149, 2005.

[14] Y. Pan, H. Xie, and G. K. Fedder, "Endoscopic optical coherence tomography based on a microelectromechanical mirror," *Opt. Lett.*, vol. 26, pp. 1966–1968, 2001.

[15] J. M. Zara, S. Yazdanfar, K. D. Rao, J. A. Izatt, and S. W. Smith, "Electrostatic micromachine scanning mirror for optical coherence tomography," *Opt. Lett.*, vol. 28, pp. 628–630, 2003.

[16] P. H. Tran, D. S. Mukai, M. Brenner, and Z. Chen, "*In vivo* endoscopic optical coherence tomography by use of a rotational microelectromechanical system probe," *Opt. Lett.*, vol. 29, pp. 1236–1238, 2004.

[17] Y. Wang, M. Bachman, G. P. Li, S. Guo, B. J. F. Wong, and Z. Chen, "Low-voltage polymer-based scanning cantilever for *in vivo* optical coherence tomography," *Opt. Lett.*, vol. 30, pp. 53–55, 2005.

[18] D. McCormick and N. Tien, "Multiple layer asymmetric vertical comb-drive actuate trussed scanning mirror," in *Proc. IEEE/LEOS Optical MEMS*, Aug. 2003.

[19] G. J. Tearney, B. E. Bouma, and F. G. Fujimoto, "High-speed phase- and group-delay scanning with a grating-based phase control delay line," *Opt. Lett.*, vol. 22, pp. 1811–1813, 1997.

Woonggyu Jung received the B.S. degree in electronics engineering from the Kyungnam University, South Korea and the M.S. degree in sensor engineering from the Kyungpook National University, South Korea, in 1999 and 2001, respectively. He is currently working in the Beckman Laser Institute and toward the Ph.D. degree in biomedical engineering, University of California, Irvine.

His research interests include 3-D optical coherence tomography, endoscopic probe and optical MEMS device.

Jun Zhang received the Ph.D. degree on optics from Shanghai Jiaotong University, China, in 2001. He joined as a Postdoctoral Researcher of Beckman Laser Institute at University of California, Irvine, in 2002.

Dr. Zhang's research is focused on the development of optical coherence tomography (OCT), Fourier domain optical coherence tomography (FDOCT), optical Doppler tomography (ODT) and polarization sensitive optical coherence tomography (PS-OCT).

Lei Wang, photograph and biography is not available at the time of publication.

Petra Wilder-Smith is an Associate Professor and Director of Dentistry at the Beckman Laser Institute and Medical Clinic, University of California, Irvine. She is also Adjunct Assistant Professor at Loma Linda University Dental School, and Visiting Professor at Aachen University in Germany. She has been working with lasers since 1985, and is interested in imaging, diagnostic and therapeutic applications of lasers. Current projects include noninvasive diagnosis of premalignancy and malignancy, noninvasive imaging and diagnostics of biofilms, holographic measurement and "impression" techniques, noninvasive detection of periodontal disease activity, applications of lasers in endodontics and periodontics, and photodynamic diagnosis and therapy of biofilms and of malignancy. She has pioneered the noninvasive measurement of pulpal and periodontal blood flow and its relation to clinical and therapeutic parameters.

Dr. Wilder-Smith is an Honorary Fellow of UCI Cancer Center.

Zhongping Chen (M'03) received the Ph.D. degree in applied physics from Cornell University, Ithaca, NY, in 1992.

He joined the Beckman Laser Institute, University of California, Irvine, in 1995 and is currently a Professor of Biomedical Engineering at UC, Irvine. He also holds a joint faculty appointment in the Department of Electrical Engineering and Computer Science and Department of Surgery. He has published more than 70 peer-reviewed papers and review articles and holds a number of patents in the fields of biomaterials, biosensors, and biomedical imaging. His research interests encompass the areas of biomedical photonics, microfabrication, biomaterials, and biosensors. His group has developed a noninvasive technology, known as phase resolved functional optical coherence tomography, which allows cross-sectional imaging of tissue structure, blood flow, and birefringence simultaneously with high spatial resolution. His current research focuses on integrating advanced optical and microfabrication technology with biotechnology for the development of biomedical diagnostic and therapeutic devices.

Dr. Chen is a fellow of American Institute of Medical and Biomedical Engineering.

Daniel T. McCormick received the B.S.E. degree in biomedical engineering and electrical engineering from Duke University, Durham, NC, in 1999, and the M.S. and Ph.D. degrees in electrical and computer engineering from Cornell University, Ithaca, NY, in 2002 and 2003, respectively. His doctoral dissertation focused on microelectromechanical systems (MEMS) for *in vivo* optical coherence tomography imaging and radio frequency (RF) applications.

Since graduation, he has been a Postdoctoral Associate Researcher in the Berkeley Sensor and Actuator Center at the University of California, Berkeley, continuing his research on the RF and biomedical applications of MEMS. He is also with the Adriatic Research Institute, Berkeley, where he is a Microsystems Engineer and a Course Instructor. His research interests also include integration of MEMS and microelectronics for high-precision instrumentation.

Norman C. Tien (S'87–M'89) received the B.S. degree from the University of California, Berkeley, the M.S. degree from the University of Illinois, Urbana–Champaign, and the Ph.D. degree from the University of California, San Diego.

He is Professor and Chair of the Department of Electrical and Computer Engineering at the University of California, Davis. His research is in microelectromechanical systems (MEMS), particularly for application in information technology. He has a joint appointment as Professor of Electrical Engineering and Computer Science, at U.C. Berkeley and is also a Co-Director of the Berkeley Sensor & Actuator Center (BSAC). He was on the faculty at Cornell University from 1996 to 2000, where he became Associate Professor in the School of Electrical and Computer Engineering.

Dr. Tien is a National Science Foundation (NSF) CAREER Award recipient. He is an editor of the IEEE/ASME JOURNAL OF MICROELECTROMECHANICAL SYSTEMS.